Journal of Alloys and Compounds 480 (2009) 727–731

Contents lists available at ScienceDirect

Journal of Alloys and Compounds

journal homepage: www.elsevier.com/locate/jallcom

Study of calcium doping effect on thermophysical properties of some perovskite manganites

Renu Choithrani [a,*], N.K. Gaur [a], R.K. Singh [b]

[a] Department of Physics, Barkatullah University, Bhopal, MP – 462 026, India
[b] School of Basic Sciences, MATS University, Raipur, CG – 492 002, India

ARTICLE INFO

Article history:
Received 20 November 2008
Received in revised form 21 January 2009
Accepted 10 February 2009
Available online 23 February 2009

PACS:
74.25.Bt
75.47.Lx
75.80. +q

Keywords:
CMR materials
Rare earth alloys and compounds
Heat capacity
Thermophysical properties

ABSTRACT

We have computed the effect of calcium doping on thermophysical properties of some perovskite manganites: $Nd_{0.04}Sm_{0.16}Ca_{0.8}MnO_3$ and $Pr_{1-x}Ca_xMnO_3$ ($0.3 \le x \le 0.5$) using a modified rigid ion model (MRIM) in the temperature range 2 K $\le T \le$ 300 K. The trends of variation of our computed specific heats with temperature are in agreement with corresponding experimental data for almost all the compositions (x) with minor deviations at higher temperatures. The specific heats are found to increase with temperature from 2 to 300 K, while they decrease with concentration (x) for these perovskite manganites. These features are exhibited by both the experimental and our theoretical results. In addition, we have used MRIM to compute the thermodynamical parameters whose results are discussed in detail for the present system of manganites.

1. Introduction

There has been enormous interest in the study of the physical properties of $Nd_{0.04}Sm_{0.16}Ca_{0.8}MnO_3$ and $Pr_{1-x}Ca_xMnO_3$ ($0.3 \le x \le 0.5$) and related rare-earth perovskite manganites due to their colossal magnetoresistance (CMR) behavior [1]. However, very scant attention has been focused on the specific heat measurements, while it is regarded as a useful technique for the study of thermophysical properties. At high temperatures, specific heat data probes the nature of magnetic, structural and electronic phase transitions. At low temperatures, the data yields information on lattice, electronic and magnetic excitations [2]. Thus, the thermophysical properties of rare earth manganites with general formula $R_{1-x}A_xMnO_3$, (R is trivalent rare earth ion; A is a divalent alkaline-earth ion) have attracted considerable attention in current years. The electronic, transport, ferromagnetic and CMR properties depend on the concentration of Mn^{+4} ions, which are created by the substitution of trivalent R ions with divalent A ions. These manganese oxides exhibit the semiconducting behavior in the paramagnetic phase and the metallic behavior in the ferromagnetic state near *Tc* [3,4].

The physical properties of manganese perovskites arise from the strong competition among the ferromagnetic double exchange interaction, antiferromagnetic superexchange interaction and spin-phonon coupling. These interactions are determined by the intrinsic parameters such as the doping level, average cationic size, cationic disorder, and oxygen stoichiometry. The simultaneous presence of Mn^{+4} and Mn^{+3} ions in these manganites leads to the double exchange mechanism and accounts for the appearance of the ferromagnetism and accompanied semiconductor-to-metal transition. However, several reports have pointed out that the role played by the electron-phonon interaction mediated by the Jahn–Teller distortion due to Mn^{+3} ion environment is important. The recently developed CMR materials are useful for various applications [5], such as those related the ferroelectric thin films, microwaves, spintronics, semiconductor technologies, data storage devices etc.

The crystal structure of given manganites with space group *pnma* has an orthorhombic structure having four formula units per unit cell with four 3d electrons: three t_{2g} and one e_g electrons showing marked CMR effect. Particularly in $Nd_{0.04}Sm_{0.16}Ca_{0.8}MnO_3$, the transition from paramagnetic to antiferromagnetic state is accompanied by a structural transformation from an orthorhombic *pnma* phase to a monoclinic $P2_1/m$ phase [4].

Among the doped manganites, $Pr_{1-x}Ca_xMnO_3$ ($0.3 \le x \le 0.5$) compounds are especially fascinating as they are paramagnetic insulators at high temperatures and undergo a charge ordering (CO)

* Corresponding author. Tel.: +91 755 2745677; fax: +91 755 2677723.
E-mail address: renuchoithrani@gmail.com (R. Choithrani).

0925-8388/$ – see front matter © 2009 Elsevier B.V. All rights reserved.
doi:10.1016/j.jallcom.2009.02.034

transition at $T_{CO} \approx 230$ K for the composition range $0.3 \le x \le 0.5$. An antiferromagnetic (AFM) ordering occurs below T_{CO} with Neel temperatre (T_N) changing from 180 ($x = 0.5$) to 140 K ($x = 0.3$) [6]. For $x = 0.37$ composition, the charge and orbital ordering occurs at $T_{CO} \approx 235$ K, while a long-range AFM order sets in only below $T_N \approx 170$ K [7].

Among the recently developed technological materials, manganites are convenient candidates for both the experimental and theoretical studies, because their physical properties in the vicinity of the phase transitions, or otherwise, are strongly affected by the fields applied to study them (such as temperature, pressure, electric, and magnetic fields). Therefore, we have investigated the temperature dependence of thermophysical properties of $Nd_{0.04}Sm_{0.16}Ca_{0.8}MnO_3$ and $Pr_{1-x}Ca_xMnO_3$ ($0.3 \le x \le 0.5$) compounds. The specific heat, as a fundamental thermophysical quantity, is complementary to the magnetic and transport properties. In this paper, we have described the specific heat and thermodynamic parameters of $Nd_{0.04}Sm_{0.16}Ca_{0.8}MnO_3$ and $Pr_{1-x}Ca_xMnO_3$ ($0.3 \le x \le 0.5$) manganites in detail using the modified rigid ion model (MRIM) developed by us [8–11].

The formulation of the interaction potential of MRIM has been elaborated in Section 2. The computed results are presented and discussed in the next section.

2. Formalism of MRIM and computational method

The formalism of MRIM has been derived from the following interatomic interaction potential [8–11];

$$\phi = \frac{e^2}{2}\sum_{kk'} Z_k Z_{k'} r^1_{kk'} + \left[nb_1 \beta_{kk'} \exp\left\{\frac{r_k + r_{k'} - r_{kk'}}{\rho_1}\right\} + \frac{n'}{2} b_2 \left[\beta_{kk} \exp\left\{\frac{2r_k - r_{kk}}{\rho_2}\right\} + \beta_{k'k'} \exp\left\{\frac{2r_{k'} - r_{k'k'}}{\rho_2}\right\}\right]\right] - \sum_{kk'} c_{kk'} r^6_{kk'} - \sum_{kk'} d_{kk'} r^8_{kk'} \quad (1)$$

The symbols involved in it are the same as those defined in our earlier papers [8]. Here, k (k') denote the positive (negative) ions and the sum is taken over all the ions (kk'). $\beta_{kk'}$ are the Pauling coefficients expressed as:

$$\beta_{kk'} = 1 + \left(\frac{z_k}{n_k}\right) + \left(\frac{z_{k'}}{n_{k'}}\right) \quad (2)$$

with z_k ($z_{k'}$) and n_k ($n_{k'}$) as the valence and number of electrons in the outermost orbits of k (k') ions and $r_{kk'}$ and r_{kk}(=$r_{k'k'}$) are the first and second neighbour ion separations, respectively. In Eq. (1), the first term represents the long-range Coulomb attraction, the second and third terms are the short-range Hafemeister-Flygare [12] type repulsion operative upto the second neighbour ions. The fourth and fifth terms in it are the vdW energies due to the dipole–dipole (d–d) and dipole-quadrupole (d–q) interactions with $c_{kk'}$ and $d_{kk'}$ as the corresponding vdW coefficients. The values of these coefficients are determined by using the following expressions

$$c_{kk'} = \left(\frac{3e^2\alpha_k\alpha_{k'}}{2m}\right)\left[\left(\frac{\alpha_k}{N_k}\right)^{1/2}\left(\frac{\alpha_{k'}}{N_{k'}}\right)^{1/2}\right]^{-1} \quad (3)$$

$$d_{kk'} = \left(\frac{27e^2\alpha_k\alpha_{k'}}{8m}\right)\left[\left(\frac{\alpha_k}{N_k}\right)^{1/2} + \left(\frac{\alpha k'}{N_{k'}}\right)^{1/2}\right]^2 \times \left[\left(\frac{\alpha_k}{N_k}\right)^{1/2} + 20/3\left(\frac{\alpha_k\alpha_{k'}}{N_k N_{k'}}\right)\left(\frac{\alpha_{k'}}{N_{k'}}\right)\right]^{-1} \quad (4)$$

derived from the Slater-Kirkwood Variational (SKV) method [13]:

Here, m and e are the mass and charge of electrons, respectively. $\alpha_k(\alpha_{k'})$ are the polarizabilities of $k(k')$ ions; N_k ($N_{k'}$) are the effective number of electrons responsible for the polarization of $k(k')$ ions. The values of $c_{kk'}$ and $d_{kk'}$ are evaluated using the Eqs. (3) and (4) and following the procedure prescribed by us [8–11].

The hardness (b) and range (ρ) parameters are determined from the equilibrium condition:

$$\left[\frac{d\phi(r)}{dr}\right]_{r=r_0} = 0 \quad (5)$$

and the expression for the bulk modulus:

$$B = (9Kr_0)^{-1}\left[\frac{d^2\phi(r)}{dr^2}\right]_{r=r_0} \quad (6)$$

Here, K is the crystal structure constant and r_o is the equilibrium interatomic separation.

The specific heat of the doped manganites is calculated using the following expression [8]:

$$C = 9R\left(\frac{T}{\theta_D}\right)^3 \int_0^{\theta_D/T} \frac{e^x X^4}{e^x - 1} dx \quad (7)$$

Here, the notations involved have the same meaning as defined in our earlier papers [8].

Besides, we have computed the cohesive energy (ϕ), molecular force constant (f), compressibility (β), Restrahalen frequency (υ_0), Debye temperature (θ_D) and Grüneisen parameter (γ) for $Nd_{0.04}Sm_{0.16}Ca_{0.8}MnO_3$ and $Pr_{1-x}Ca_xMnO_3$ ($0.3 \le x \le 0.5$) compounds using their expressions given in our earlier papers [8–11]. The results thus obtained are presented and discussed below.

3. Results and discussion

We have evaluated the model parameters (b, ρ) from Eqs. (5) and (6) by taking the values of the input data (r_0, B_T) directly from Refs. [4,6–7,14–17] and the vdW coefficients ($c_{kk'}$ and $d_{kk'}$) estimated from SKV method [13]. The values of computed model parameters (b_1, ρ_1 and b_2, ρ_2) corresponding to Mn–O and R–O bonds at room temperature for $Nd_{0.04}Sm_{0.16}Ca_{0.8}MnO_3$ and $Pr_{1-x}Ca_xMnO_3$ ($0.3 \le x \le 0.5$) are listed in Table 1. Using these values of model parameters, we have computed the cohesive energy (ϕ), molecular force constant (f), compressibility (β), Restrahalen frequency (υ_0), Debye temperature (θ_D) and Grüneisen parameter (γ) by using their expressions reported by us [8–11]. The computed results on them are listed in Table 2 and some of them are found to be in somewhat good agreement with the experimental data [7,18,19] available only for the composition ($x = 0.5$).

The cohesive energy is the measure of strength of forces binding the atoms together in solids. The cohesive energy is, therefore, expected to follow the same trend of variations as that of the compressibility, which represents the resistance to the volume change and is related to the overall atomic binding properties of a material. In conformity with this, we notice from Table 2 that our results on

Table 1
The model parameters of $Nd_{0.04}Sm_{0.16}Ca_{0.8}MnO_3$ and $Pr_{1-x}Ca_xMnO_3$ ($0.3 \le x \le 0.5$).

Compounds	Model parameters			
	Mn–O		R/Ca–O	
	b_1 (10^{-12} erg)	ρ_1(Å)	b_2 (10^{-12} erg)	ρ_2 (Å)
$Nd_{0.04}Sm_{0.16}Ca_{0.8}MnO_3$	1.124	0.386	1.271	0.541
$Pr_{0.70}Ca_{0.30}MnO_3$	1.119	0.421	1.414	0.634
$Pr_{0.65}Ca_{0.35}MnO_3$	1.311	0.462	1.615	0.654
$Pr_{0.63}Ca_{0.37}MnO_3$	1.512	0.482	1.816	0.680
$Pr_{0.55}Ca_{0.45}MnO_3$	1.713	0.493	2.017	0.689
$Pr_{0.50}Ca_{0.50}MnO_3$	1.914	0.524	2.218	0.699

Table 2
Thermophysical properties of $Nd_{0.04}Sm_{0.16}Ca_{0.8}MnO_3$ and $Pr_{1-x}Ca_xMnO_3$ ($0.3 \le x \le 0.5$).

Compounds	ϕ (eV)	f (10^4 dyne. cm^{-1})	β (10^{-12} dyn^{-1} cm^2)	υ_0 (THz)	Θ_D (K)	γ
$Nd_{0.04}Sm_{0.16}Ca_{0.8}MnO_3$	−142.425	11.712	3.021	8.903	425.80	2.17
$Pr_{0.70}Ca_{0.30}MnO_3$	−143.992	13.147	3.132	9.516	455.14	2.21
$Pr_{0.65}Ca_{0.35}MnO_3$	−144.546	13.228	3.144	9.597	459.01	2.24
$Pr_{0.63}Ca_{0.37}MnO_3$	−144.792	13.492	3.152	9.661	462.07	2.28
$Pr_{0.55}Ca_{0.45}MnO_3$	−145.619	13.571	3.161	9.739	465.80	2.32
$Pr_{0.50}Ca_{0.50}MnO_3$	−145.994	13.642	3.170	9.768	467.21	2.41
(Expt.)	(−141.810)[a]	–	–	(9.790)[b]	(470)[b]	(2–3)[c]

[a] Ref. [18].
[b] Ref. [7].
[c] Ref. [19].

the cohesive energy (ϕ) have followed more or less the same trend of variation as that exhibited by the compressibility. Nevertheless, they are stable compounds as the cohesive energy is negative within the studied range of temperature and composition (x). Due to the lack of experimental data, we have compared the cohesive energy of the present compounds with the parent member $LaMnO_3$ [18] of this family.

The Restrahalen frequencies (υ_0) for $Nd_{0.04}Sm_{0.16}Ca_{0.8}MnO_3$ and $Pr_{1-x}Ca_xMnO_3$ ($0.3 \le x \le 0.5$) are listed in Table 2 and found to increase with concentration (x) and this feature is similar to the increasing trends exhibited by both the hardness (b_1, b_2) and the stability ($-\phi$) of the present materials. Further, this frequency varies with the concentration of Mn^{+4} ions which are created by the substitution of trivalent R ions with divalent A ions. The calculated Restrahalen frequency (=9.661 THz) for $Pr_{0.63}Ca_{0.37}MnO_3$ is in agreement with the experimental data (=9.79 THz) [7] available only for $Pr_{0.63}Ca_{0.37}MnO_3$. It is also seen from Table 2 that our theoretical values of Grüneisen parameters (γ) for $Nd_{0.04}Sm_{0.16}Ca_{0.8}MnO_3$ to $Pr_{1-x}Ca_xMnO_3$ ($0.3 \le x \le 0.5$) are lying between 2 and 3, which are similar to those as reported by Dai et al [19].

The computed results on Debye temperatures (θ_D) obtained from MRIM for $Pr_{1-x}Ca_xMnO_3$ ($0.3 \le x \le 0.5$) from MRIM are closer to the experimental data (θ_D = 470 K) available only for x = 0.37 [7] at room temperature. The higher values of Debye temperatures indicate the higher phonon frequencies of these compounds. It is interesting to note from Table 2 that the computed values of Debye temperatures of $Nd_{0.04}Sm_{0.16}Ca_{0.8}MnO_3$ and $Pr_{1-x}Ca_xMnO_3$ ($0.3 \le x \le 0.5$) are between 425.80 and 467.21 K, which lie within the Debye temperature range (300–550 K) often found in the perovskite manganites. For the present system of manganites, we could compare our results, listed in Table 2, with experimental data available only for the composition x = 0.37. Most of these results are, probably, being reported for the first time and hence they are of academic interest at present, but they will serve as a guide to the experimental workers in future.

The temperature dependence of the computed and measured specific heats (C) for $Nd_{0.04}Sm_{0.16}Ca_{0.8}MnO_3$ and $Pr_{1-x}Ca_xMnO_3$ ($0.3 \le x \le 0.5$) compounds are depicted in Figs. 1–4 in the range 2 K $\le T \le$ 300 K. It is noticed from the Fig. 1 that the computed specific heat curve for $Nd_{0.04}Sm_{0.16}Ca_{0.8}MnO_3$ is in agreement with the experimental data [4] and the trends of variations exhibited by the experimental and theoretical results are almost similar except for the strong peak shown by the measured data at ~150 K. This observed peak owes its origin to the occurrence of the charge and orbital ordering effects in the manganites. However, this peak could not be reproduced from our theoretical results due to the exclusion of the charge and ordering effects in MRIM.

It is seen from Figs. 2–4 that the specific heats (C) are decreasing with the increase of doping Ca (x = 0.3 to 0.5) in $PrMnO_3$. The change of Mn–O distance by the substitution of Ca at Pr site increases Debye temperature (θ_D) and hence there is a sharp decrease in the specific

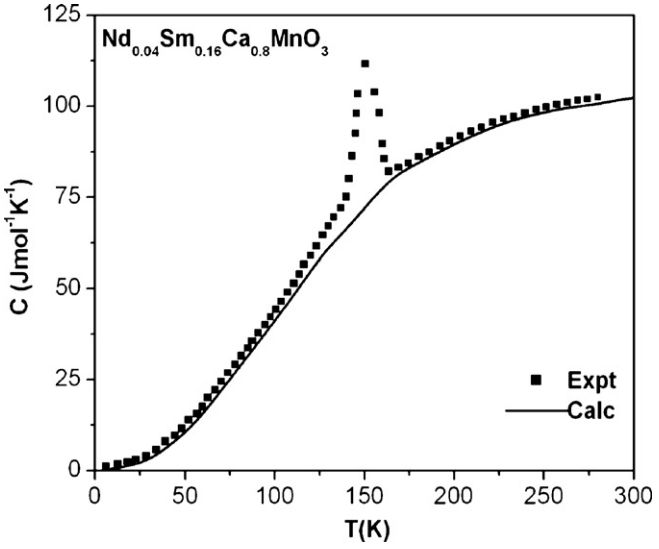

Fig. 1. The variation of specific heat of $Nd_{0.04}Sm_{0.16}Ca_{0.8}MnO_3$ with temperature, where solid line (—) and the squares (■) are the present theoretical and the experimental [4] results, respectively.

heat values on Ca doping in $PrMnO_3$ and this feature is demonstrated by plotting C (2 K) against x in Fig. 5. It is also seen from Figs. 2 (a, b) and 4 (a, b) that the present theoretical results on specific heats have shown the trends similar to those exhibited by the

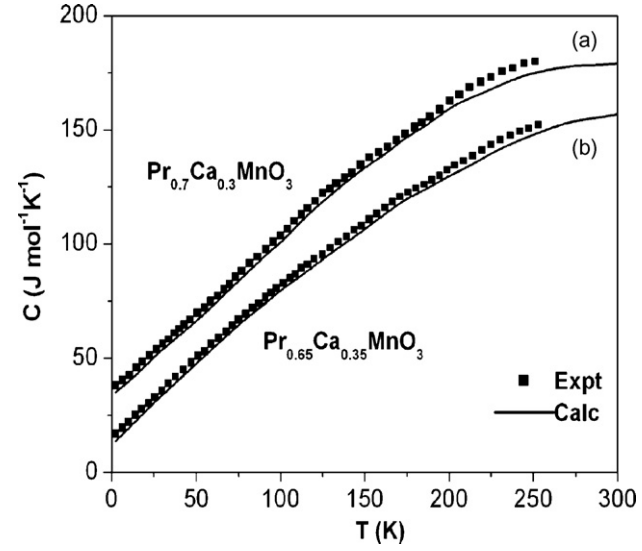

Fig. 2. (a, b) The variation of specific heat of $Pr_{0.70}Ca_{0.30}MnO_3$ and $Pr_{0.65}Ca_{0.35}MnO_3$ with temperature, where solid lines (—) and the squares (■) are the present theoretical and the experimental [6] results, respectively.

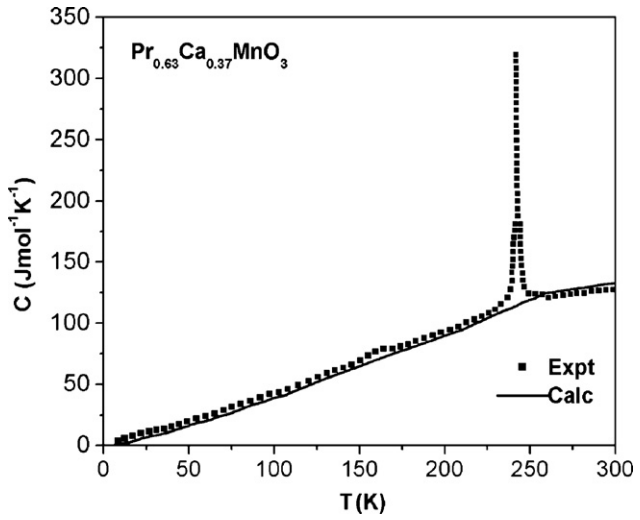

Fig. 3. The variation of specific heat of $Pr_{0.63}Ca_{0.37}MnO_3$ with temperature, where solid line (—) and the squares (■) are the present theoretical and the experimental [7] results, respectively.

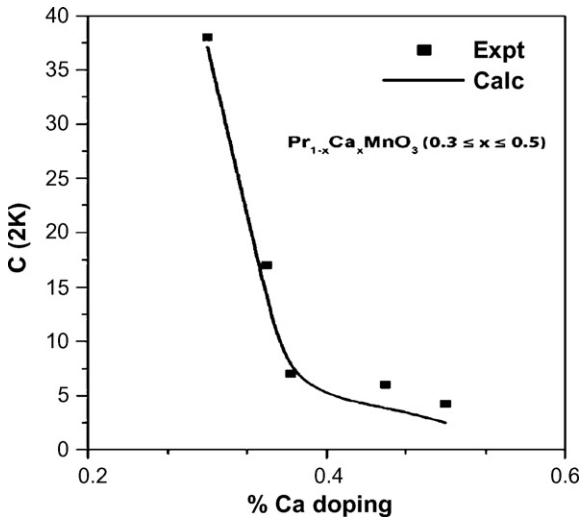

Fig. 5. The variation of the specific heat, $C(2K)$, with composition (x) in $Pr_{1-x}Ca_xMnO_3$ ($0.3 \le x \le 0.5$). The solid line (—) is the present theoretical and the squares (■) are experimental [6,7] results.

experimental data [6]. However, the marked deviations between the theoretical and experimental results at higher temperatures from 150 to 250 K might be due to the exclusion of anharmonic effects in MRIM framework. The specific heat increases with the increase of temperature in $Pr_{1-x}Ca_xMnO_3$ for all the compositions ($0.3 \le x \le 0.5$). It is also important to note from the Figs. 1–4 that the specific heats at $2\,K \le T \le 300\,K$ show a significant decrease (as shown in Fig. 5 for C (2K)) due to the doping of calcium in these perovskite manganites. This doping of Ca, in turn, oxidizes Mn^{+3} to Mn^{+4} that introduces the holes into the d-band and hence gives rise to some interesting features in their physical properties.

The measured specific heats [7] in $Pr_{0.63}Ca_{0.37}MnO_3$ have revealed a sharp peak (see Fig. 3) at around 235 K. This might be due to the occurrence of the charge and orbital ordering effects at $T_{CO} \approx 235$ K, while a long-range AFM ordering sets in around $T_N \approx 170$ K. However, both the peaks are not revealed from our theoretical results. This might be so because we have not included the charge and ordering effects in our model (MRIM) as mentioned earlier.

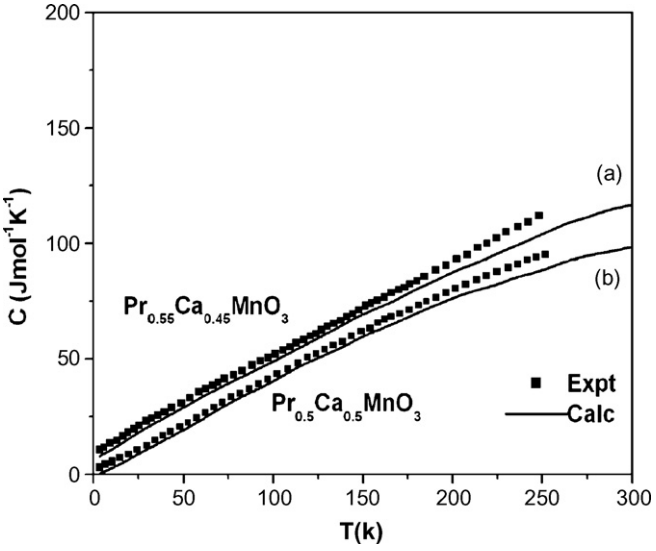

Fig. 4. (a,b). The variation of specific heat of $Pr_{0.55}Ca_{0.45}MnO_3$ and $Pr_{0.50}Ca_{0.50}MnO_3$ with temperature, where solid lines (—) and the squares (■) are the present theoretical and the experimental [6] results, respectively.

4. Conclusion

The success of the modified rigid ion model (MRIM) in describing the thermophysical properties of the structurally complex system of perovskite manganites may be considered remarkable in view of its inherent simplicity. The sharp peaks observed in specific heat data on $Nd_{0.04}Sm_{0.16}Ca_{0.8}MnO_3$ ($T \approx 150$ K) and $Pr_{0.63}Ca_{0.37}MnO_3$ ($T \approx 235$ K) could not be reproduced from MRIM results due to the exclusion of charge and ordering effects in this model. Since the specific heat studies illustrate the role of theoretical models for the prediction of macroscopic thermodynamic properties and several other interesting physical features, therefore, MRIM seems to be an appropriate model for describing the thermophysical properties of pure and doped perovskite manganites. Also, it is obvious that MRIM has a potential to describe the cohesive, thermodynamic and physical properties of solids and alloys. The MRIM results, which could not be compared due to the lack of experimental data on thermodynamic parameters, will serve as a guide to the experimental workers in future.

Acknowledgement

One of the authors (Renu Choithrani) would like to acknowledge with thanks for the generous financial support and the award of Senior Research Fellowship (SRF) by the Council of Scientific and Industrial Research (CSIR), Government of India, New Delhi.

References

[1] T. Kimura, G. Lawes, T. Goto, Y. Tokura, A.P. Ramirez, Phys. Rev. B 71 (2005) 224425.
[2] L. Ghivelder, I. Abrego Castillo, N.McN. Alford, G.J. Tomka, P.C. Riedi, J. MacManus-Driscoll, A.K.M. Akther Hossain, L.F. Cohen, J. Magn. Magn. Mater. 189 (1998) 274.
[3] H. Takashi, M. Mohammad, F. Adrian, M. Adriana, Y. Seiji, D. Elbio, Phys. Rev. Lett. 90 (2003) 247203.
[4] D.A. Filippov, R.Z. Levitin, A.N. Vasil'ev, T.N. Voloshok, R. Suryanarayanan, Physica B 327 (2003) 155.
[5] E.E. Rodriguez, Th. Proffen, Llobet, Ryne, Phys. Rev. B 71 (2005) 104430.
[6] V.N. Smolyaninova, A. Biswas, X. Zhang, K.H. Kim, Bog-Gi Kim, S-W. Cheong, R.L. Greene, arXiv: cond-mat/0004180v1 [cond-mat.str-el], 11 April 2000.
[7] A.K. Raychaudhuri, A. Guha, I. Das, R. Rawat, C.N. Rao, Phys. Rev. B 64 (2001) 165111.
[8] Renu Choithrani, N.K. Gaur, R.K. Singh, Solid State Commun. 147 (2008) 103; N.K. Gaur, Renu Choithrani, A. Srivastava, Solid State Commun. 145 (2008) 308.

[9] Renu Choithrani, N.K. Gaur, R.K. Singh, J. Phys. : Condens. Matter. 20 (2008) 415201.
[10] Renu Choithrani, N.K. Gaur, J. Magn. Magn. Matter. 320 (2008) 612.
[11] Renu Choithrani, N.K. Gaur, J. Magn. Magn. Matter 320 (2008) 3384.
[12] D.W. Hafemiester, W.H. Flygare, J. Chem. Phys. 43 (1965) 795.
[13] J.C. Slater, K.G. Kirkwood, Phys. Rev. Lett. 37 (1931) 682.
[14] K.S. Nagapriya, A.K. Raychaudhuri, Bhavtosh Bansal, V. Venkataraman, Sachin Parashar, C.N.R. Rao, Phys. Rev. B 71 (2005) 024426.
[15] J. Hemberger, M. Brando, R. Wehn, V.Yu. Ivanov, A.A. Mukhin, A.M. Balbashov, A. Loidl, Phys. Rev. B 69 (2004) 064418.
[16] J.G. Cheng, Y. Sui, X.J. Wang, Z.G. Liu, J.P. Miao, X.Q. Huang, Z. Lu, Z.N. Qian, W.H. Su, J. Phys. : Condens. Matter. 17 (2005) 5869.
[17] A. Oleaga, A. Salazar, D. Prabhakaran, A.T. Boothroyd, J. Phys. : Condens. Matter. 17 (2005) 6729.
[18] R. De Souza, M. Saiful Islam, E.I. Tiffe, J. Mater. Chem. 9 (1999) 1621; N.N. Kovalova, J.L. Gavartin, A.L. Shluger, A.M. Stoneham, Physica B 734 (2002) 312.
[19] P. Dai, Z. Jiandi, H.A. Mook, S.H. Lion, P.A. Dowben, E.W. Plummer, Phys. Rev. B 54 (1996) R3694.